



Jurnal Pertahanan

Media Informasi tentang Kajian dan Strategi Pertahanan yang Mengedepankan *Identity*, *Nationalism* dan *Integrity*

e-ISSN: 2549-9459

<http://jurnal.idu.ac.id/index.php/DefenseJournal>



DESIGN AND IMPLEMENTATION OF ANTI-TANK GUIDED-MISSILE (ATGM) CONTROL SYSTEM USING SEMI-AUTOMATIC COMMAND LINE OF SIGHT (SACLOS) METHOD BASED ON DIGITAL IMAGE PROCESSING

Muhammad Hanifudin Al Fadli¹, Dadang Gunawan², Romie Oktovianus Bura³

The Republic of Indonesia Defense University
IPSC Sentul, Bogor, West Java, Indonesia 16810

hanifudinmuhammad@idu.ac.id¹, dadang.gunawan@idu.ac.id², romiebura@idu.ac.id³

Larasmoyo Nugroho⁴

National Institute of Aeronautics and Space
Rocket Technology Center, Bogor, West Java

larasmoyo@yahoo.com⁴

Article Info

Article history:

Received :
February 14, 2021
Revised :
June 30, 2021
Accepted :
August 22, 2021

Keywords:

Anti-Tank Guided Missile,
Image Processing,
Infrared,
Raspberry Pi,
SACLOS.

Abstract

The Anti-Tank Guided-Missile (ATGM) system has a very important role in the modern battlefield. This system proved its effectiveness in many modern conflicts such as the Syrian Civil War and Nagorno-Karabakh War. The ATGM system has a very simple electronic and mechanism but it has a very high level of accuracy and precision. One of the control methods used in ATGM is SACLOS method. This method tracks missile position by detecting an infrared lamp that is placed on the missile tail. The tracking system sends control signals to the missile as a result of the correction of the missile position when flying. The infrared tracking system in this research was made using a modified OV5647 camera with the addition of a 940 nm narrow bandpass filter. There are 3 cameras with 1x, 8x, and 16x magnifications which are accessed using 3 Raspberry Pi boards. X and y coordinate data of the infrared lamp is sent to the airframe using wireless telemetry. Atmega328 microcontroller process x and y coordinate data into input proportional control. The result of this research is the prototype of an anti-tank missile control system with an infrared tracking instrument capable track a series of 88 infrared LEDs as far as 997.16 meters with a tracking speed of 90.11 FPS. The threshold parameters of image processing using luminance of YUV color space has a range of 240-255. The control parameter $K_p=7$ is used in wind tunnel testing with airspeed 20 m/s capable of directing airframe motion to the telescope's crosshairs.

DOI:

<http://dx.doi.org/10.33172/jp.v7i2.755>

© 2021 Published by Indonesia Defense University

INTRODUCTION

The Anti-Tank Guided-Missile (ATGM) is a missile that is specifically designed to destroy the tank and other armored vehicles. ATGM has many improvements of method and control system so its make many generations. The various types of ATGM control systems are (Gander, 2000):

1. Manual Command Line of Sight (MCLOS). This is the first generation of the ATGM control system. The operator uses a joystick to control the direction of the missile when it's moving towards the target. The control signal is sent from the joystick on the launcher side to the missile using a cable, for example, 9k11.
2. Semi-Automatic Command Line of Sight (SACLOS). The operator keeps the telescope crosshair to the target to be hit. The missile will fly along the crosshairs, so the missile's flight moves toward the target indirectly. There are 3 types of anti-tank missile control using the SACLOS method:
 - a. Lamp/Flare: Infrared lamp or flare is placed on the tail of the missile. The infrared tracking system tracks the position of the missile when flying by tracking the infrared lights. The position of the infrared lamp is used as a feedback signal to control the direction of the missile's flight along the crosshairs, for example, Konkurs, Metis, Fagot, and Milan.
 - b. Laser Beamriding: Gunner transmits a laser beam directed toward the target. The laser beam is modulated so the laser receiver placed on the tail of the missile can receive the beam and translate it into flight control commands. The missile will fly in the laser beam area towards the target, for example, Ingwee, Kornet, Konus, Kombat, Falarick, Khrizantema, Shershen, and Ataka.
 - c. Laser Illuminator: A laser illuminator illuminate the target with an infrared laser that is modulated at a certain frequency. The laser receiver sensor placed on the nose of the missile will

guide the missile towards the target, for example, Hellfire and Cirit.

3. Fire and Forget (Lock On Before Launch). The third-generation anti-tank missiles use the infrared electro-optical camera as an image processing sensor. The camera is placed on the nose of the missile to lock on the target. When the target is locked, the missile will fly t the target and the gunner can leave the launch site, for example, Javelin.
4. Fire and Update (Lock On After Launch). The fourth-generation anti-tank missile is the same as the third generation in principle, but after firing the missile, the gunner can update the target because the missile is connected with the launcher using fiber optic cable, for example, Spike and Raybolt.

The SACLOS method has better accuracy and precision than MCLOS. The SACLOS method is also a unique system. Unlike the Fire and Forget or Fire and Update method that place an expensive infrared camera as a seeker system in the missile section, the SACLOS method uses an infrared seeker that tracks infrared lamp/flare. The infrared seeker in the SACLOS method is placed in the launcher section, not in the missile section, so the seeker is not destroyed when the missile hits the target. Because of this unique system, the SACLOS method has a cheaper price comparing to the Fire and Forget or Fire and Update.

Several research of ATGM control systems is "Fuzzy Controller for Antitank Wire Guided Missile Simulator with Direct X SDK" which was done by Valentine Penev. This study uses a missile launcher as a media interface for operators and monitors to display shooting scene scenes in 3D visually (Penev, 1999). On research titlef "Programmed Control of the Flat Track Anti-Tank Guided Missile" carried out by Zbigniew Koruba and Lukasz Nocon, the SACLOS control system algorithm was developed so that the missile was able to hit targets that were not visible in line of sight provided that the target

position had known the initial position and did not move (Koruba & Nocon, 2014).

Kresimir Cosic, Ivica Kopriva, Todor Kostic, Miroslav Slamic dan Marijo Volarevi conducted a study or research titled “Design and Implementation of A Hardware-In-Loop Simulator for A Semi-Automatic Guided Missile System” implements hardware in loop SACLOS control system based on Texas Instrument TMS320C40 board. A computer was used to simulate the SACLOS missile control system at distances of 100 to 2000 meters. An A3 size plotter is used to simulate the movement of the missile (Ćosić, Kopriva, Kostić, Slamić, & Volarević, 1999).

This study aims to design and implement of ATGM control system using SACLOS method based on digital image processing. Many current ATGM systems using single detector analog infrared seekers that operate in Medium Wave Infrared (MWIR) or Long Wave Infrared (LWIR) wavelength. In this research, the seeker is made from a modified commercial OV5647 camera that operates in Near-Infrared 940 nm wavelength. By accessed using digital image processing, the analog noise environment can be eliminated. Digital image processing also offers convenience in the improvement of the control system and tracking system because all of the parameters can be changed by software.

METHODS

The infrared light tracking system is designed using a modified OV5647 camera with the addition of a 940 nm narrow bandpass filter. There are 3 cameras with 1x, 8x, and 16x magnifications which are accessed using 3 Raspberry Pi boards. The output of the Raspberry pi is the x, y coordinates and the width and height of the infrared lamp placed on the airframe model.

Data from each Raspberry Pi is sent to the Atmega2560 microcontroller via serial communication. The function of the Atmega2560 microcontroller is to select data from the Raspberry Pi board. Atmega2560 microcontroller then sends x and y coordinate data to the Atmega328 microcontroller using 433 MHz telemetries. Atmega328 microcontroller process the x-axis error and y-axis error into proportional control input that is used to drive 3 servos on the tail fin so the direction of the airframe model is moved to the midpoint of the OV5647 camera crosshairs. A 3-9x32 Bushnell telescope is mounted parallel to the OV5647 camera so that the missile operator only needs to keep the telescope's midpoint towards the target and the control system automatically guides the direction of the airframe's model towards the target. The operational concept of the missile system is shown in Figure 1.

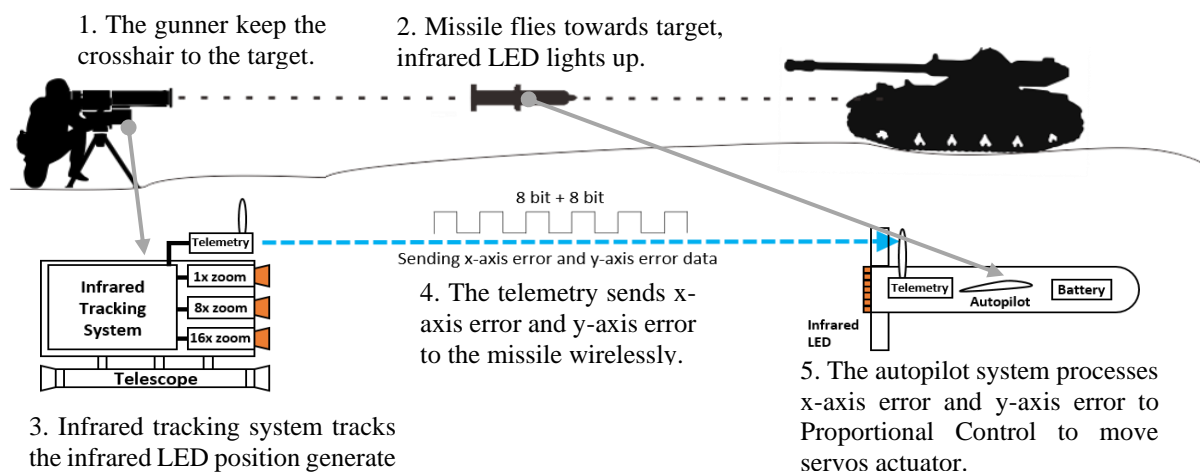


Figure 1. The operational concept of the missile system.
 Source: Processed by Author, 2019.

Airframe Model Hardware Design

The airframe model is designed both in 2D and 3D. The airframe model is made from a 5 mm polyfoam board. The airframe model hardware design is shown in Figure 2.

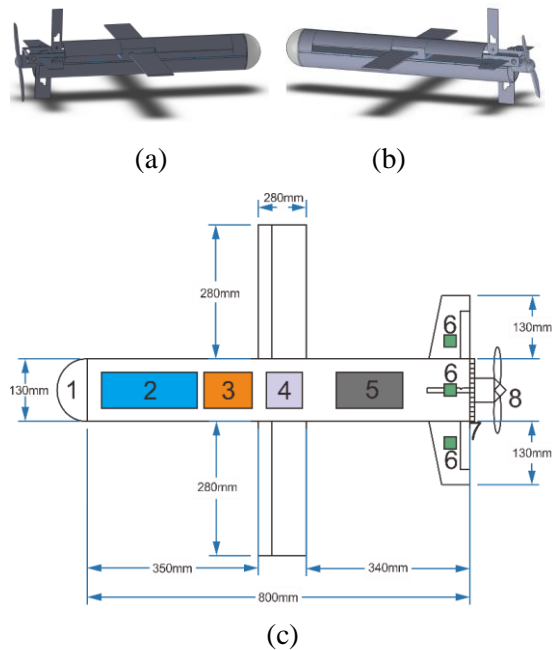


Figure 2. (a) (b) (c) Mechanical design and loads placement of airframe model.
Source: Processed by Authors, 2019.

The parts of the model airframe along with an explanation of each device are as follows:

1. Radome: Front cover of the airframe model and to keep the aerodynamic airflow along with the airframe model.
2. Battery: The source of power supply for the electronic airframe model system. The battery used is Lithium Polymer 4S 2200 mAh.
3. Microcontroller: Main control of the electronic system airframe model. The microcontroller used is the Atmega328 running at 16 MHz.
4. Sensor block: There are gyroscope accelerometer MPU-6050 and magnetometer HMC5883.
5. ESC: Electronic Speed Controller is a brushless motor control speed device
6. Servo Motor: Electric tail fin actuator.
7. Infrared Light Emitting Diode (LED) circuit: The circuit is a series of infrared

LED 940 nm. There is a total of 88 pieces of LED's, arranged 10 pieces in the series circuit and 8 pieces in the parallel circuit.

8. Brushless motor: Electric propulsion system of airframe model. The Brushless motor used is 1400 KV and 10x5E propeller.

Design of Airframe Model Electronic System

The electronic system used for autopilot is based on the Atmega328 8-bit microcontroller. The microcontroller run in 16 MHz crystal. The schematic of the Atmega328 microcontroller circuit is shown in Figure 3.

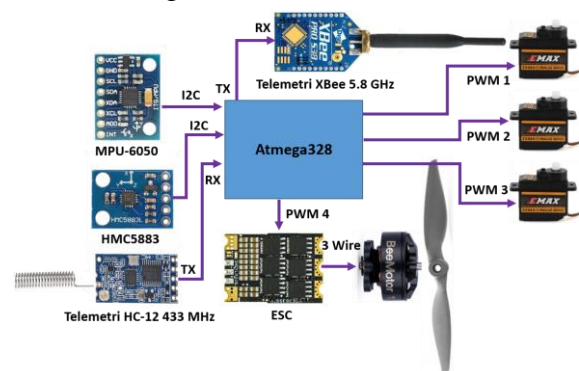


Figure 3. Atmega328 microcontroller circuit schematics.
Source: Processed by Authors, 2019.

Interface descriptions of each component are:

1. MPU-6050: Inertial Measurement Unit (IMU) gyroscope sensor and accelerometer. Used to read airframe pitch and roll angles. Accessed using the Inter-Integrated Circuit (I2C) at address 0xD0 (Inversense Inc, 2013).
2. HMC-5883: IMU sensor magnetometer. Used to read the yaw angle of the airframe. Accessed using I2C at address 0x3C (Honeywell International Inc, 2013).
3. Telemetry HC-12: Telemetry 433 MHz to receive x and y coordinate data on infrared lights from the gunner electronic block. Accessed using the serial interface (Silicon Laboratories, 2016).

4. Xbee Telemetry: 2.4 GHz telemetry to transmit IMU parameters and the x and y coordinates of the infrared lamp from the airframe model to the computer. This X Bee Telemetry is accessed using serial interface communication (Digi International Inc, 2009).
5. Servo Motor: Model airframe tail fin actuator. Accessed using a 20 ms Pulse Width Modulation (PWM) signal with high signal variations of 1-3 ms at port C.0 to port C.2 on Atmega328 controller.
6. ESC: Brushless motor driver. Accessed using a 20 ms PWM signal with high signal variations of 1-3 ms at port C.3.

Design of Atmega328 Microcontroller Program

The program used on the Atmega328 microcontroller is written in the C programming language. The algorithm used on the Atmega328 microcontroller is shown in Figure 4.

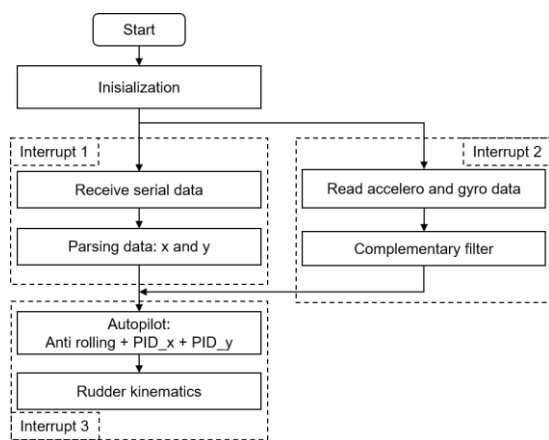


Figure 4. Atmega328 microcontroller algorithm flowchart.

Source: Processed by Authors, 2019.

The program uses 3 interrupt routines. The first interrupt is used to receive serial data from HC-12 telemetry. The second interrupt is used to read the gyroscope, accelerometer, and magnetometer then combined using the complementary filter for better measurement (Asrofi, Sumardi, &

Setiyono, 2015). The third interrupt is used to process the proportional control signal then forward it into servo motor movement.

Design of Infrared Lamp Tracking Instrument

The infrared lamp tracking electronic system was designed using a modified OV5647 camera with the addition of a 940 nm narrow bandpass filter lens. There are 3 cameras with a magnification of 1x, 8x, and 16x. Each camera is accessed using the Raspberry Pi board. A schematic of an infrared lamp-tracking electronic circuit system is shown in Figure 5.

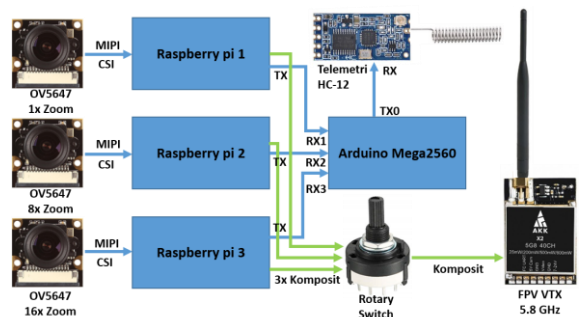


Figure 5. Schematic of electronic systems for tracking infrared lights.

Source: Processed by Authors, 2019.

The interface description of each component is as follows:

1. OV5647: Used as an imaging infrared camera sensor. Accessed using Camera Serial Interface (CSI-2) cable.
2. Raspberry Pi: Mini computer for digital image processing.
3. Atmega2560 microcontroller: x, y, w, h data selector of each Raspberry Pi. The selector can be selected automatically and manually using a rotary switch.
4. Rotary Switch: Manual input selector for the Atmega2560 microcontroller and composite video signal.
5. HC-12 telemetry: Transmit data from the infrared tracking system to the airframe model. Accessed using the serial interface.
6. Video Transmitter (VTX): Transmit composite video signals to the computer.

Design of Raspberry Pi Program

All of this Raspberry Pi runs on the Linux Raspbian Operating System. OpenCV library program was installed in Raspberry Pi board with Python language interpreter. The software is designed to run automatically when the power supply is turned on and can be turned off by pressing the turn-off button. The algorithm used on the Raspberry Pi board is shown in Figure 6.

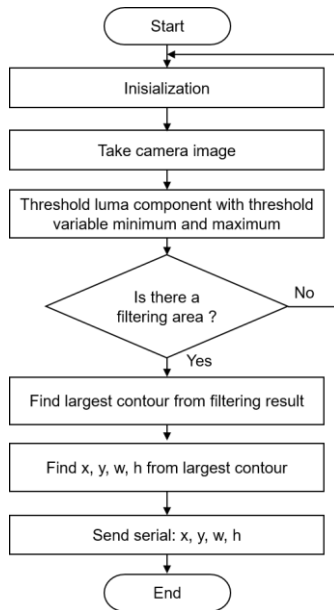


Figure 6. Raspberry Pi algorithm flowchart. *Source:* Processed by Authors, 2019.

The image processing method used in this research is thresholding color in YUV color space. YUV color space consists of Y that represents the luma component, U represent blue chrominance, and V represents the red chrominance. The results of the thresholding are then sorted. If there is more than one infrared lamp, the contour with the largest area is selected. The coordinate values x, y, w, and h from the largest area contour are sent to the Atmega2560 microcontroller via serial communication.

Raspberry Pi Graphical User Interface (GUI) is designed to show tracking parameters in a real-time tracking process. There is information such as x, y, w, h coordinate, tracking time, Frame per Second (FPS) speed, IP address, and

processing time. The Raspberry Pi display is shown in Figure 7. Information about digital image processing data processed by Raspberry Pi is displayed on a GUI display of 320x240 pixels.



Figure 7. Raspberry Pi interface display. *Source:* Processed by Authors, 2019.

Design of Atmega2560 Microcontroller Program

Atmega2560 microcontroller is programmed using the C programming language. Atmega2560 is used for the data selector from 1x zoom, 8x zoom and 16x zoom cameras. The selector process can be selected in automatic mode using a filter size w and h infrared lights parameters or manual mode using a rotary switch knob.

X and y data are sent to the airframe model using HC-12 433 MHz telemetry. The algorithm used on the Atmega2560 microcontroller is shown in Figure 8.

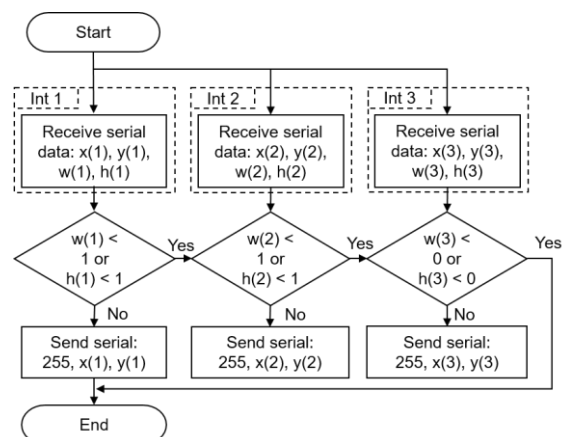


Figure 8. Atmega2560 microcontroller program algorithm. *Source:* Processed by Authors, 2019.

The filters used in the auto-selector algorithm are the width filter and height filter. If the width and height of the infrared light image is less than 1 pixel, the

Atmega2560 microcontroller will automatically select the serial data from the smaller optical zoom to the bigger optical zoom.

Explanation of Communication Interface

Three main system blocks are used in this research, the airframe model block, the gunner block, and the data acquisition block. All of these blocks are separated in distance from each other, so communication between blocks must be done wirelessly. The communication interface between blocks is shown in Figure 9. The 433 Mhz communication is carried out on the gunner block and the airframe model block. The device is an HC-12 telemetry module. This communication function is to send x and y coordinate data from the gunner block to the airframe model block wirelessly.

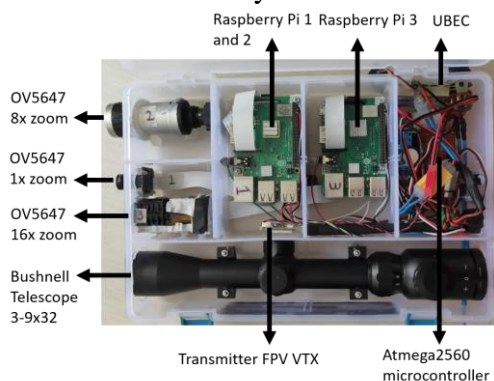


Figure 9. Communication interface between blocks.

Source: Processed by Authors, 2019.

The airframe model sends the data to the acquisition system using the Xbee telemetry 2.4 GHz communication module. The data is x, y, w, h data from image processing and roll, pitch, yaw data from IMU sensors processing. The gunner electronic block sends the Raspberry Pi tracking video via 5.8 GHz communication to the computer. This communication is done by Video Transmitter Eachine module and received by RC832 module. The UTV-007 adapter with STK1160 chip is used to convert analog video data to Universal

Serial Bus (USB) data, so the video can be displayed on computer Graphical User Interface (Syntek Semiconductor Co. Ltd, 2006).

Design of Gunner Interface

The gunner sees the target through the 3-9x32 Bushnell telescope. The gunner can adjust the telescope magnification manually from 3x to 9x zoom. To shoot a target, the gunner must keep the telescope's crosshair toward the target. The telescope's crosshairs are calibrated with the OV5647 camera's viewfinder so they are aligned to each other. The placement of the telescope and OV5647 camera in the infrared light tracking system is shown in Figure 10.

The optoelectronic infrared tracking system block is placed in a Lionstar brand plastic box with dimensions of 30x18x6 cm. The infrared tracking system block is placed on the tripod holder. The mechanics of tracking an infrared lamp using a tripod are shown in Figure 11.

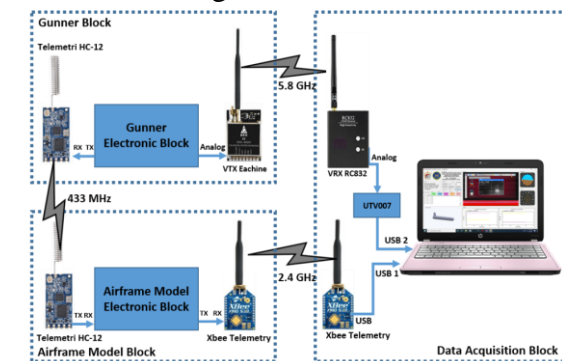


Figure 10. Placement of the 3-9x32 Bushnell telescope on the infrared tracking system block.

Source: Processed by Authors, 2019.



Figure 11. Placement of an electronic block tracking system of infrared lights on a tripod

Source: Processed by Authors, 2019.

Design of Infrared Lamp Circuit

The infrared lamp which used are LED with the center wavelength of 940 nm, diameter size 5 mm, and bandwidth wavelength 45 nm (Everlight, 2005). 10 LEDs arranged in series with the additional 86 Ohm resistor. There are 8 series of LED series arranged in parallel so the total number of LEDs used is 88 lamps. The schematic of the LED light circuit is shown in Figure 12.

The LED circuit is placed on the tail section of the airframe. The placement of the LED lighting circuit on the airframe is shown in Figure 13. 88 infrared LED is connected in half circle Printed Circuit Board (PCB). It can be done because there is a brushless motor placed in the body center axis of the airframe, so the dimension must be fitted.

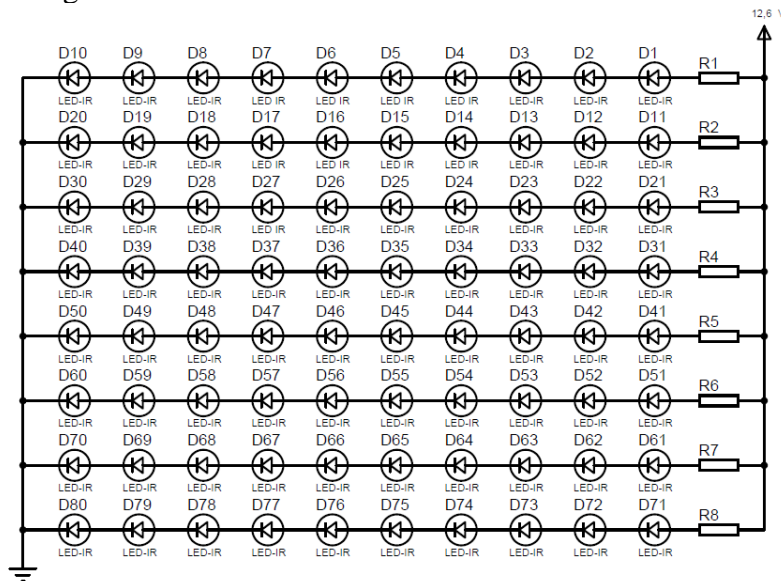
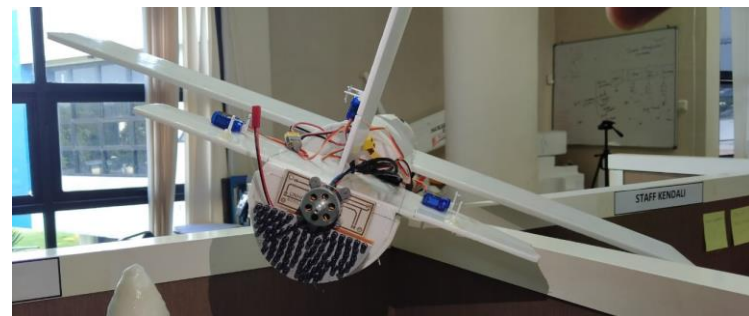


Figure 12. Schematic of 88 infrared LEDs.

Source: Processed by Authors, 2019



(a)



(b)

Figure 13. (a) (b) Placement infrared LED circuit on the airframe.

Source: Processed by Authors, 2019.

RESULT AND DISCUSSION

After designing and implementing a missile control system on hardware, it is necessary to test. The tests were carried out in two ways, the partial test and the overall test. A partial test is done to find out the performance of each component. The overall test is done by testing the control system implemented on the airframe model in the wind tunnel.

Testing YUV Color Space Thresholding Parameters

The color space that used in this research is YUV parameters. The testing of YUV parameters was carried out using infrared LED lights 940 nm 5 mm in diameter from a distance of 50 cm. The test is carried out in sunny conditions. Thresholding values are true if the results of the thresholding show white on the infrared light and black on the environment frame. The results of threshold YUV values are shown in Figure 14.

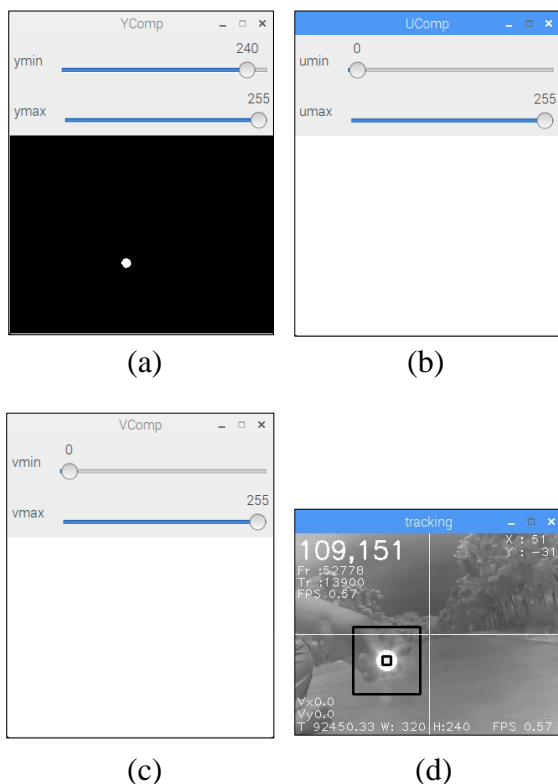


Figure 14. The results of thresholding parameters (a) Y, (b) U, (c) V and (d) windows tracking result display.

Source: Processed by Authors, 2019.

Threshold parameters of U and V values cannot distinguish between infrared LED light and the environment light condition because the image detected by the camera is a grayscale image with 940 nm wavelength, so it has no blue (U) and red (V) components. The image only has a luminance value (Y). The threshold parameter of YUV is shown in Table 1.

Table 1. Value of YUV threshold parameters.

No	Parameter	Min	Max	Range
1	Y	240	255	15
2	U	-	-	-
3	V	-	-	-

Source: Processed by Authors, 2019.

The threshold parameters used in this digital image processing are only the Y parameter, while the U parameter and V parameter are not used because they do not have any effect on image processing.

Testing of Color Robustness

These tests were carried out to determine the robustness of the OV5647 camera against light sources that emit light color at different wavelength spectrums. The red color has a wavelength of 635-700 nm, the green color has a wavelength of 490-560 nm, and the blue color has a wavelength of 450-490 nm (Bharadwaj, 2014). An example of infrared sensor testing for a blue light source is shown in Figure 15.



Figure 15. (a) Image of a blue LED light taken from a normal camera (distance of 50 cm). (b) The image of the blue LED light is taken from the OV5647 camera (50 cm distance).

Source: Processed by Authors, 2019.

Three of the visible light color space spectrum is tested in the OV5647 camera. The red LED, the green LED and the blue LED is turned on by the CR2032 3V battery in front of the OV5647 camera at a 50 cm distance. The Raspberry Pi board takes video from OV5647 via a CSI-2 connector. The results of the OV5647 camera's robustness testing with other light sources are shown in Table 2. Test results on various light sources that have different colors show that the OV5647 camera has the robustness to the red, green, and blue light sources.

Table 2. Result of OV5647 robustness testing with other light sources.

No	Color Test LED -	Result
1	IR 940 nm	Detected
2	Red	Not detected
3	Green	Not detected
4	Blue	Not detected

Source: Processed by Authors, 2019.

Testing of Raspberry Pi FPS Speed

FPS is the number of images processed in one second. The method to calculate FPS speeds is to count the number of images processed by Raspberry Pi divided by time in units of seconds. The FPS speed test results for each camera are shown in Table 3.

Table 3. Raspberry Pi FPS test result.

Test no -	Raspi 1x Zoom	Raspi 8x Zoom	Raspi 16x Zoom
1	90	90.16	90.15
2	90	90.17	90.16
3	90.01	90.15	90.20
4	90.02	90.15	90.15
5	90.02	90.16	90.15
Avg	90.01 FPS	90.16 FPS	90.16 FPS

Source: Processed by Authors, 2019.

The average speed of the Raspberry Pi FPS with a 1x optical zoom camera is 90.01 FPS, 8x optical zoom is 90.16 FPS, and 16x optical zoom is 90.16 FPS. The maximum FPS speed of the OV5647 camera is 120 FPS (OmniVision Technologies Inc., 2009)

Testing of Camera Detection Range

The test is carried out to determine the detection distance of each camera against the infrared LED circuit. The test was carried out in the field of the Lapan Rocket Technology Center and Gunung Maloko Street Rumpin Bogor. An example of testing an infrared camera's detection distance at a distance of 345.39 meters is shown in Figure 16.

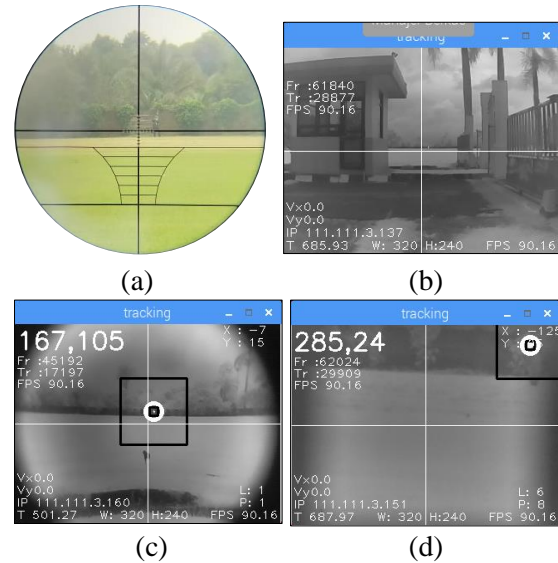


Figure 16. (a) Testing view from the Bushnell 9x32 telescope (b) Testing view from the OV5647 1x zoom (c) Testing view from the OV5647 8x zoom (d) Testing view from the OV5647 16x zoom from distance of 345.39 meters.

Source: Processed by Authors, 2019.

At a distance of 345.39 meters, a series of the infrared LED circuit were not detected from a 1x magnification OV5647 camera. At the same distance, a series of infrared LED circuits detected 1x1 pixels from an 8x zoom camera and detected 8x6 pixels from a 16x zoom camera. The maximum detection of the OV5647 camera to the infrared LED circuit is shown in Table 4.

The maximum detection test of OV5647 with 1x zoom is 85.71 meters, maximum detection test of OV5647 with 8x zoom is 435.11 meters, and maximum detection test of OV5647 with 16x zoom is 997.16 meters.

Table 4. Maximum detection test of OV5647 camera.

No	OV5647 Camera zoom -	Range (m)
1	1x	85.71
2	8x	435.11
3	16x	997.16

Source: Processed by Authors, 2019.

Testing of Inertia Measurement Unit

IMU sensor testing is carried out to determine the magnitude of the measurement error using a protractor and the calculation of the IMU sensor reading. The range of measurement angles for roll and pitch airframe models is limited to the range of -45° to +45° and the yaw angle in the range 0-360°. The difference in the reading and measurement values of the IMU sensor is shown in Figure 17.

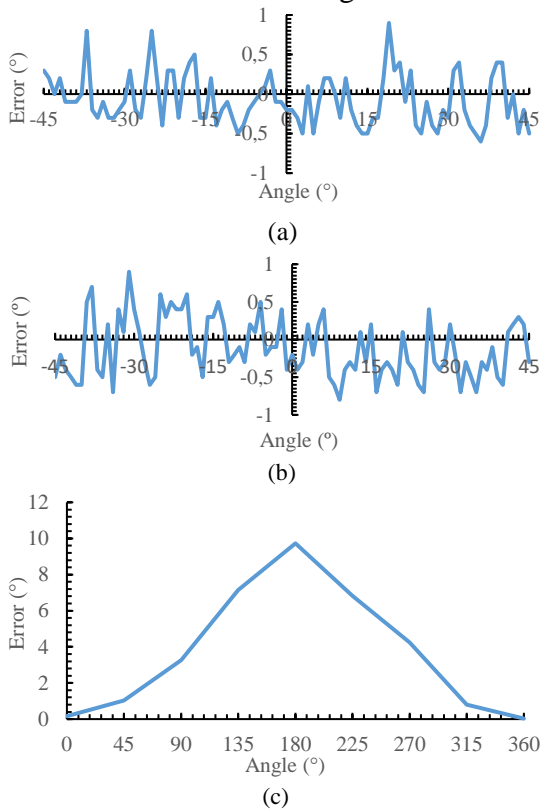


Figure 17. (a) Graph of pitch angle error (b) Graph of roll angle error (c) Graph of yaw angle airframe model.

Source: Processed by Authors, 2019.

The average error value of airframe pitch measurement and calculation results is 0.29°, the roll angle is 0.37°. Yaw angle errors slowly rise from 0° to 180° then slowly go down to 360°. The maximum

error value is 9.37°. Yaw angle errors occur because the HMC5883 sensor placement is not on the airframe rotary axis.

Testing of Servo Control Signal

Servo control signals use a 20 ms PWM signal with high logic signal variations of 1-2 ms (Prayogo, Triwiyatno, & Sumardi, 2018). There are 3 servos placed on the tail fin. The design of the servo control signal is shown in Figure 18.

To change the control signal from low logic signal to high logic signal using Timer 1 Overflow and to pull down using Compare A Match on signal 1 and Compare B Match on signal 2. Testing the timing signal of the motor servo is done by comparing the input signal with the output signal measured using an oscilloscope. Changing in timing value of 100 μs results in a change in servo angle of 10° with a value of 0° at a time of 1.5 ms (Al Fadli, Riyadi, & Setiyono, 2018). The results of testing the servo motor timing signals are shown in Table 5. The angular error that occurs in each motor servo is no more than 1°.

Table 5. Testing of motor servo signal timing.

No	Device	Error signal (μs)		Error angle (°)	
		Min	Max	Min	Max
1	Servo 1	-10	30	0	1
2	Servo 2	0	20	0	0.5
3	Servo 3	0	10	0	1

Source: Processed by Authors, 2019.

Testing of The Overall System

The test is done by hanging the airframe model using a rope in the wind tunnel at Rocket Technology Center LAPAN Bogor with a wind speed of 20m/s and a proportional constant parameter Kp=7. Based on IMU sensor testing and image processing error values, a rule base can be formulated as follows:

$$kinematics(x, y, \psi, \theta) \left\{ \begin{array}{l} \text{if } x \gg \ominus \text{ then } \psi \gg \oplus \\ \text{if } x \gg \oplus \text{ then } \psi \gg \ominus \\ \text{if } y \gg \ominus \text{ then } \theta \gg \ominus \\ \text{if } y \gg \oplus \text{ then } \theta \gg \oplus \end{array} \right.$$

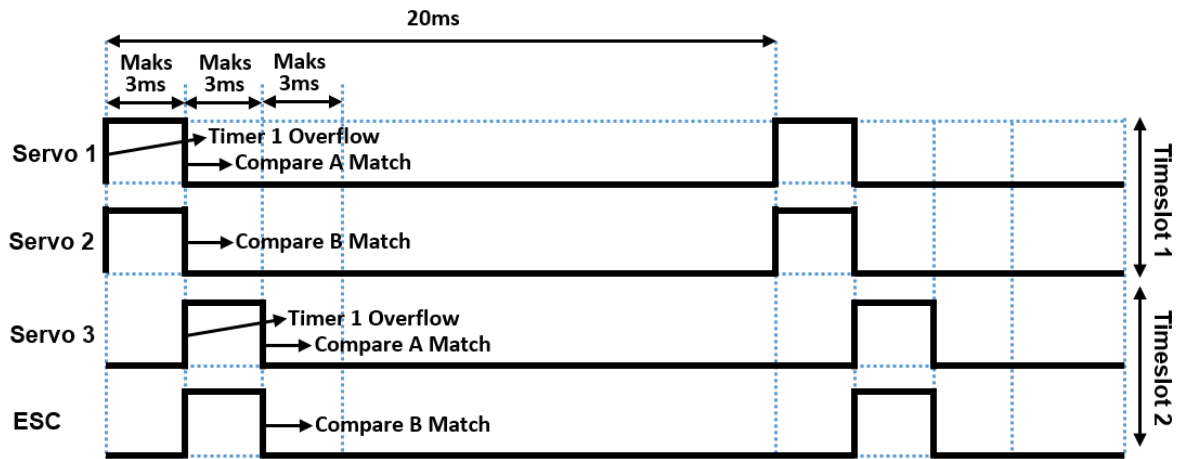


Figure 18. Servo motor timing signals.
 Source: Processed by Authors, 2019.



Figure 19. Testing airframe model in the LAPAN wind tunnel.
 Source: Processed by Authors, 2019.

The change in the x-axis error value of image processing is inverse to the change in the value of yaw. If the value of x decreases, the value of yaw will increase, and if the value of x increases, the value of yaw will decrease. The change in the value of the y-axis error is direct to the change in pitch value. If the y value decreases, the pitch value decreases and if the y value increases, the pitch value will increase. Figure testing airframe models in the wind tunnel are shown in Figure 19.

The test was carried out using 2 experiments, the x-axis error variation, and the y-axis error variation experiment. The x-axis error variation experiment was carried out by moving the rotate lever

towards the pan on the tripod mount of the infrared LED tracking system. The results of testing the airframe control system model in the wind tunnel varying the value of x are shown in Figure 20.

The blue lines indicate the x-axis error. It is used as feedback for the proportional control system implemented in the airframe model. The initial yaw angle value is 17.2°. When the x-axis error is shifted to the positive direction (left direction), then the yaw angle of the airframe model moves towards the negative (left direction). Shifting the left tripod causes the direction of the left airframe to move. When the x-axis error is shifted towards the negative (right direction), then the yaw angle of the

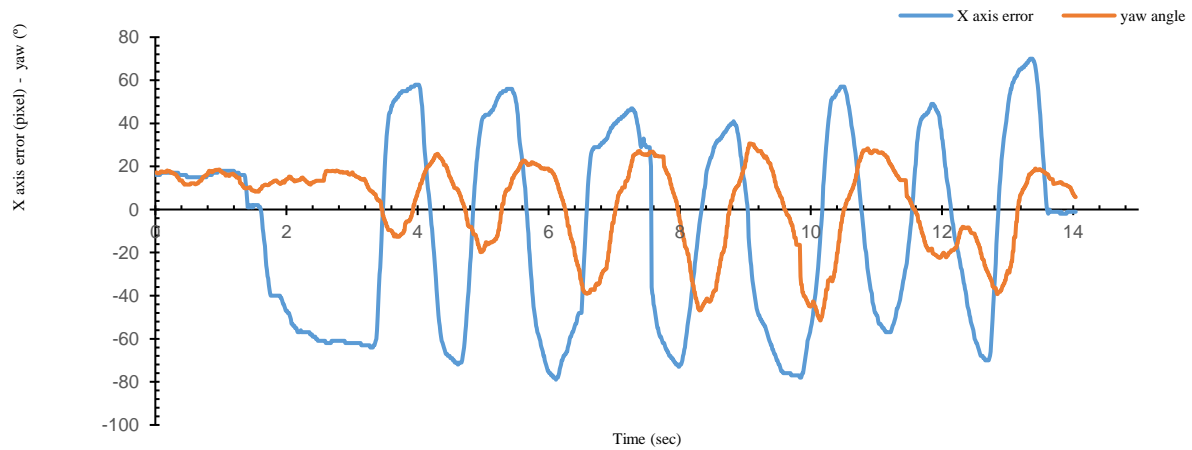


Figure 20. Graph of testing airframe models in wind tunnels with variations in x value.
Source: Processed by Authors, 2019.

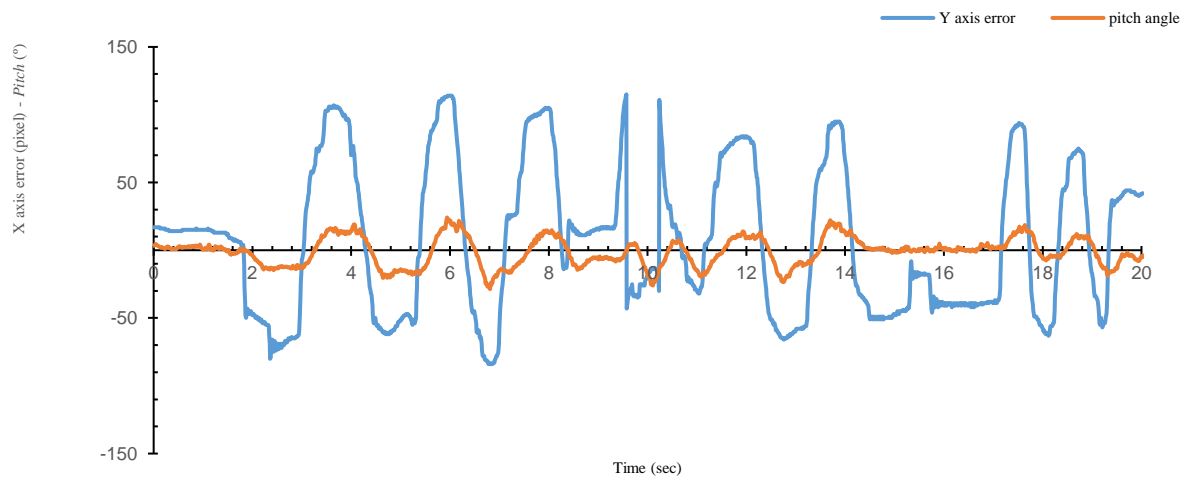


Figure 21. Graph of testing airframe models in wind tunnels with variations in y value.
Source: Processed by Authors, 2019.

airframe model moves towards the positive (right direction), so that the infrared LED light tracking system and the x-axis airframe control system work by the rule base. Furthermore, the airframe model is tested in a wind tunnel with variations in the y-axis error. The results of testing airframe models in wind tunnels at various y-axis errors are shown in Figure 21.

Blue lines indicate the y-axis error. It is used as feedback for the proportional control system implemented in the airframe model. Variation of the y-axis error is done by sliding the rotate lever towards the tilt on the tripod mount of the infrared LED

tracking system. The initial pitch angle value is 3.89° .

When the y-axis error is shifted towards the negative (upward direction), then the airframe pitch angle value moves towards the negative (upward direction). Shifting the tripod up causes the model airframe to move upward. When the y-axis error is shifted in a positive direction (downward), the airframe pitch angle value moves towards the positive (downward), so that the infrared LED light tracking system and the y-axis airframe control system work by the rule base.

**CONCLUSIONS,
RECOMMENDATION, AND
LIMITATION**

The anti-tank guided missile control system using the Semi-Automatic Command Line of Sight method was successfully implemented on the airframe model and simulated in a wind tunnel at the Bogor Lapan Rumpin Rocket Technology Center. Threshold parameter values for detecting infrared LED light circuits in the YUV color space get a minimum Y value of 240 and a maximum Y of 255. U and V parameters do not affect the detection of infrared LED lamp circuits. The average speed of image processing of the infrared LED tracking system on Raspberry Pi is 90.11 FPS. The infrared LED light tracking system can track a series of 88 infrared LED lights with a maximum detection distance of 997.16 meters. The infrared LED light tracking sensor has the robustness to the 5 mm LED light source that emits red, green, and blue light. Control parameters with a proportional control value of 7 can control airframe models in wind tunnels with wind speeds of 20 m/s.

For further development, the electronic system can be replaced using a military-grade electronic system such as FPGA or Texas Instrument for digital image processing because it has a higher data processing speed than Raspberry pi boards. The image processing algorithms can be added using the background subtraction method so they have higher robustness to environmental conditions and higher resistance to the jamming conditions.

REFERENCES

Al Fadli, M. H., Riyadi, M. A., & Setiyono, B. (2018). Perancangan Sistem Roket Kendali Berpemandu Inframerah Menggunakan Metode Pengolahan Citra Yang Disimulasikan Dalam Terowongan Angin. *Transient: Jurnal Ilmiah Teknik Elektro*, 7(1), 152–159.

Asrofi, M., Sumardi, S., & Setiyono, B.

(2015). Stabilisasi Robot Berkaki 6 (Hexapod) Pada Bidang Miring Menggunakan 9 DOF IMU Berbasis Invers Kinematic. *Transient: Jurnal Ilmiah Teknik Elektro*, 4(1), 97–105.

Bharadwaj, V. (2014). Colours: A Scientific Approach. *International Journal of Research*, 1–6. Uttarakhand: International Journal of Research.

Ćosić, K., Kopriva, I., Kostić, T., Slamić, M., & Volarević, M. (1999). Design and implementation of a hardware-in-the-loop simulator for a semi-automatic guided missile system. *Simulation Practice and Theory*, 7(2), 107–123. [https://doi.org/10.1016/S0928-4869\(98\)00027-5](https://doi.org/10.1016/S0928-4869(98)00027-5)

Digi International Inc. (2009). XBee ® /XBee-PRO ® RF Modules. *Product Manual v1.XEx-802.15.4 Protocol*, pp. 1–69. Minnetonka: Digi International Inc.

Everlight. (2005). Technical Data Sheet 5mm Infrared LED , T-1 3/4. *Everlight Electronics Co. LTD*, pp. 1–7. New Taipei: Everlight Electronics Co., Ltd.

Gander, T. (2000). *Anti-tank Weapons* (1st ed.). Ramsbury: Crowood Press.

Honeywell International Inc. (2013). *HMC5883L 3-Axis Digital Compass IC datasheet* (pp. 1–20). pp. 1–20. Plymouth: Honeywell International Inc.

Inversense Inc. (2013). *MPU-6000 and MPU-6050 Register Map and Descriptions* (Vol. 1, pp. 1–46). Vol. 1, pp. 1–46. Borregas Ave: InvenSense.

Koruba, Z., & Nocon, L. (2014). Programmed control of the flat track anti-tank guided missile. *Proceedings of the 2014 15th International Carpathian Control Conference (ICCC)*, 237–242. IEEE. <https://doi.org/10.1109/CarpathianC.C.2014.6843604>

OmniVision Technologies Inc. (2009).

- OV5647 datasheet* (pp. 6–1). pp. 6–1.
California: OmniVision
Technologies, Inc.
- Penev, V. (1999). Fuzzy Controller for Antitank Wire Guided Missile Simulator with Direct X SDK. *Information & Security: An International Journal*, 3, 79–90. <https://doi.org/10.11610/isij.0305>
- Prayogo, R. C., Triwiyatno, A., & Sumardi, S. (2018). Perancangan Robot Berkaki 4 (Quadruped) dengan Stabilization Algorithm Pada Uneven Floor Menggunakan 6-Dof Imu Berbasis Invers Kinematic. *Transient: Jurnal Ilmiah Teknik Elektro*, 7(2), 543–551.
- Silicon Laboratories. (2016). *Si4464 Datasheet*. Austin: Silicon Laboratories Inc.
- Syntek Semiconductor Co. Ltd. (2006). *STK1160 datasheet* (pp. 1–38). pp. 1–38. Hsinchu: Syntek Semiconductor Co., Ltd.